Available online at www.sciencedirect.com

SciVerse ScienceDirect

Procedia CIRP 4 (2012) 109 – 114

www.elsevier.com/locate/procedia

3rd CIRP Conference on Process Machine Interactions (3rd PMI)

Adaptive Cutting Force Control on a Milling Machine with Hybrid Axis Configuration

B. Denkena[a], F. Flöter[a]*

[a]Institut of Production Engineering and Machine Tools (IFW), Leibniz Universitaet Hannover, An der Universitaet 2, 30823 Garbsen, Germany.

* Corresponding author. Tel.:+49-511-76218162; fax: +49-511-7625115. E-mail address: floeter@ifw.uni-hannover.de.

Abstract

In the re-contouring process of aircraft engine components, the unknown geometry and inhomogeneous material properties of the workpiece are major challenges. For this reason a new repair process chain is supposed which consists of noncontact geometry identification, process simulation and NC-path planning, followed by a force controlled milling process. A new milling machine prototype is employed to ensure an effective force control loop. By use of a magnetic guided spindle slide, higher dynamics and precise tracking are enabled. Since variation of the process forces result in variable control plant characteristics, an indirect adaptive controller has been designed. Consequently, models of actuator and process are presented and the estimation of the present parameters by a recursive least square algorithm is outlined. Once the parameters are known, the control polynomials are calculated on the basis of a pole placement control approach. First experimental results of a force controlled milling process are put forward.

Keywords: milling; force control; adaptive control; magnetic guide

A_m, B_m	polynomials of the desired system transfer function
A, A_0, B, R, S, T	control polynomials
a_e	width of cut
a_p	axial depth of cut
d	deadtime (samples)
F_p	process force
F_{ref}	reference force
f	feed velocity
G_c	combined transfer function
G_{mag}	transfer function of the magnetic guide
G_p	transfer function of the milling process

I	identity matrix
K	estimation gain
K_c	cutting constants
N	number of teeth on the cutter
n	spindle speed
P	covariance matrix
T_s	discrete time control interval
$(x, y)_a$	actual position within the air gap
$(x, y)_c$	commanded position within the air gap
θ	parameter vector
λ	forgetting factor
ξ	damping ratio
φ	regressor vector

2212-8271 doi:10.1016/j.procir.2012.10.020

τ_{mag}	time constant of the magnetic guide
τ_c	time constant of the cutting process
ω_n	natural frequency of the closed loop system

1. **Introduction**

1.1. Motivation

Regeneration of complex durable goods has become a much noticed field in industry. Turbine blades of aircraft engines represent such an application, in which the classical repair process can be divided into workpiece preparation, build-up welding followed by re-contouring of the damaged areas. Thereby, re-contouring is a crucial task, demanding highest standards in surface geometry and surface integrity. Meanwhile solutions to handle unknown geometries and changing material properties have to be found.

Especially cutting forces have a major influence to the overall machining result. Not only surface roughness is profoundly influenced by cutting forces [1], also dimensional integrity can be violated by changing tool deflection due to changes in cutting forces. Furthermore, it is necessary to pay attention to sudden changes in cutting forces, which can act as a source for vibrations, by what the surface of a cost intensive turbine blade might experience severe damage.

Considering these challenges a new process chain (Fig. 1) is in development to improve the overall repair process. Starting with a noncontact, optical identification of the geometrical properties, the intended repair process is simulated and an individual NC-path is planned. The actual process offers the possibility of force control. Thereby, a new approach is pursued: A 3-axis milling center prototype with a contactless magnetic guided spindle slide facilitates implementing a cutting force control loop, which is fully independent from the conventional machine axes and their controls. Precise positioning (up to 1 µm) at high bandwidth (up to 30 Hz) are major advantages of this new approach. As a drawback, changes in cutting forces are associated with a deviation from the originally planned tool path. However, the resulting discrepancy path can be compensated via an adaptive NC-path. By sending a trigger signal by the moment of deviation, the affected NC block can be identified and repeated.

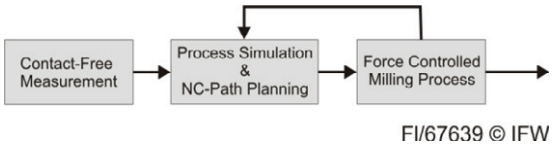

Fig 1: Intended process chain

This paper intends to show the implementation of the adaptive force control loop. It is organized as followed: In chapter 2 an overview of other adaptive cutting force control implementation is given. The consecutive chapter introduces the milling machine prototype and its hybrid axis configuration. Details of the underlying adaptive control algorithm are presented in chapter 4. The work closes with first experimental results and a conclusion.

2. **State of the Art**

In metal cutting, studies of force control have been reported for long time. Early solutions came from Koren and Masory [2, 3]. Based on the difference in reference and actual cutting force a corrective feed velocity is computed while stability of the control loop is ensured by maintaining a constant gain. Altintas presented a direct adaptive control approach [4] which is spindle speed independent and therefore suitable for combination with chatter suppression techniques based on spindle speed variations. Landers et al. compared different model based force control techniques in terms of performance and stability in [5]. Zhang and Chen found a solution for an in-process surface roughness adaptive control system [6], which aims for better surface finish. However, all approaches use the feedrate as a variable to manipulate the cutting forces.

3. **Milling Machine Prototype "Schnelle Maschine"**

To implement a force control loop which is fully independent of the conventional machine axes, a new type of milling machine is deployed. It has been developed at IFW [7, 8]. A structure of the full-size 3-axis machine tool with its components is shown in Figure 2. A linear electromagnetic guide is the distinctive feature of this prototype.

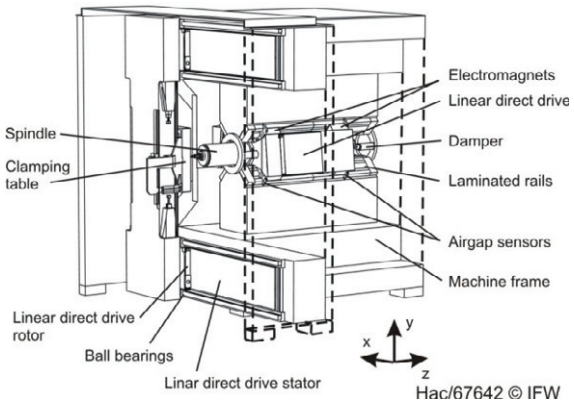

Fig 2: Machine tool prototype 'Schnelle Maschine'

The Z-axis slide, carrying the spindle, is guided by the application of the principle of magnetic levitation. This allows a completely frictionless operation of the slide within the air gap of 0.7 mm at each of the eight electromagnets.
By integration of linear direct drives in each axis, accelerations between 4.3 g and 4.7 g are possible. X- and Y-axis are guided by conventional ball bearings.

3.1. Control Structure

As an active component, the magnetic guide needs to be controlled. The air gaps at each actuator are measured and transformed into the generalized coordinates (q1,…, q5) (Fig. 3), which represent five degrees of freedom (DOF) of the slide. The sixth DOF of the body, the Z-slide's transverse direction, is controlled by a linear direct drive (Siemens 840D powerline).
A PI-state space controller, based on Kalman filtering, stabilizes the slide by calculating corrective forces at each magnet. To ensure stable operation conditions in all positions within the air gap, the nonlinear relation between air gap, current and delivered force are provided for each electromagnet. Therewith, a movement of 400µm around the center-position can be realized. The control loop runs at 5 kHz.

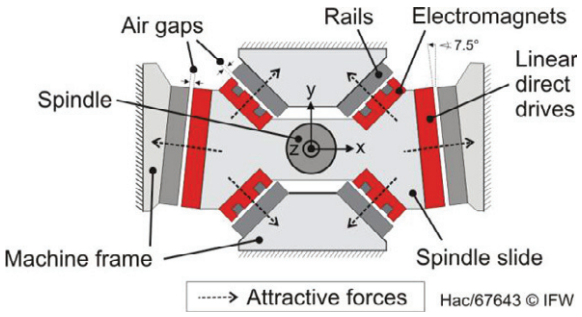

Fig. 3: Sectional view of the Z-axis

As a result of the active control of all six DOF, a dynamic relocation of the slide within the air gap becomes possible. A precision improvement by employing this technique has been presented by Kallage [9]. In terms of position control, this approach exceeds the dynamics provided by the industrial controlled direct drives [9]. Thus, the position capabilities of the Z-slide – high bandwidth and high position accuracy – are highly suited for an effective force control.

4. **Adaptive Force Control Algorithm**

An indirect pole placement control algorithm is chosen in order to constrain the cutting forces at a certain level. Models of the feed drive servo dynamics and the cutting process are set up. The unknown parameters are estimated by a recursive least square algorithm at each control step, the control polynomials are calculated and the new position command is sent to the control system of the magnetic guide.

4.1. Discrete transfer function of feed drive dynamics and cutting process

The PI-state space controller is adjusted to have almost overdamped characteristics. Thus, the positioning behavior of the magnetic guide can be modeled as a first order system plus deadtime:

$$G_{mag}(s) = \frac{(x,y)_a(s)}{(x,y)_c(s)} = \frac{1}{\tau_{mag}s+1} e^{-T_t s} \quad , \tag{1}$$

where $(x,y)_a$ and $(x,y)_c$ are the actual position and commanded position of the magnetic guide within the air gap and τ_{mag} represents the time constant of the guide. It is to note here, that G_{mag} may change. Varying the magnetic guides control system (e.g. position of the poles inside the unit circle), the rise time will be influenced.

A deviation of the complete spindle slide from its original position can be an effective way to change the cutting conditions, here the width of cut. The model described in [10] is therefore modified for a changing width of cut. Hence, the first order system illustrates as follows:

$$G_p(s) = \frac{F_p(s)}{(x,y)_a(s)} = \frac{K_c a_p f}{Nn(\tau_c s+1)} \quad . \tag{2}$$

K_c, a_p, f are representing the cutting constant, the axial depth of cut and the feed, respectively. N is the number of teeth on the cutter and n is the spindle speed. τ_c specifies the time constant of the cutting process. It is to consider, that the obtained model is not only time-variant, but also has nonlinear characteristics.
Combining (1) and (2) and transforming the resultant transfer function into discrete time domain, following simplified model is obtained:

$$G_c(z) = G_{mag}(z)G_p(z) = \frac{z^{-d}(b_0 z+b_1)}{z^2+a_1 z+a_2} \quad . \tag{3}$$

z is the forward time-shift operator and a_1, a_2, b_0, b_1 are the related coefficients. Since the magnetic guide has a deadtime of approximately one ms and the controller cycle time is 200 µsec, five time delays have to be added to the discrete time model.

4.2. Pole Placement Control Algorithm

Astrom and Wittenmark [11] presented a pole placement design procedure whereby the closed loop response of the control system performs like a desired model transfer function. A brief summary is given here. For the detailed controller design it is referred to [11].

The controller consists of a feedforward filter (T), a feedback filter (S), a regulator (R) and an observer (A_0) (Fig. 4).

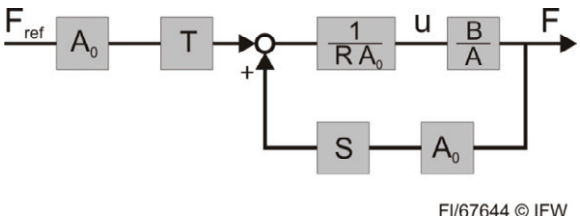

Fig. 4: Block diagram of the pole placement control system

Defining A_m and B_m as the denominator and numerator of the desired closed loop systems' transfer function, the system can be described as follows:

$$\frac{F_p}{F_{ref}} = \frac{BT}{AR+BS} = \frac{A_0 B_m}{A_0 A_m} \quad . \tag{5}$$

In this case, a second order system is chosen to represent the desired response of the control system. Hence, the z-transform displays as

$$\frac{B_m}{A_m} = \frac{1+m_1+m_2}{z^2+m_1 z+m_2} \quad , \tag{6}$$

where

$$m_1 = -2e^{-\xi\omega_n T}\cos\left(\omega_n\sqrt{1-\xi^2}T_s\right) \quad , \tag{7}$$

$$m_2 = e^{-2\xi\omega_n T} \quad . \tag{8}$$

T_s represents the discrete control interval, ξ the damping ratio and ω_n the natural frequency. Even though the zero of the machine tool plant (5) should always be stable, the estimation algorithm might provide an unstable zero. Therefore it is abstained from cancelling the process zero.

The control polynomials of (5) have to fulfill the causality rules, which have been proven in [11]. In the underlying case, they result to:

$$A_0(z) = z^{d+1} \quad , \tag{9}$$

$$R(z) = z^{d+1} + \sum_{i=1}^{d+1} r_i z^{d+1-i} \quad , \tag{10}$$

$$S(z) = \sum_{i=0}^{d+1} s_i z^{d+1-i} \quad . \tag{11}$$

The polynomial of the feedforward filter $T(z)$ can be determined by the numerator of (5). The scale factor b_{m0} in (12) thereby ensures a unity gain in the overall closed loop system.

$$T(z) = b_{m0} z^d \quad , \tag{12}$$

$$\text{with } b_{m0} = \frac{1+a_{m1}+a_{m2}}{b_0+b_1} \quad . \tag{13}$$

By solving the Diophantine equation of (5), the control polynomials can be determined. An exemplarily solution of the Diophantine equation can be found in [10].

In order to estimate the time-varying, unknown parameters of (3) which are needed to set up the control polynomials, a standard recursive least square algorithm is used.

4.3. Recursive Least Squares Parameter Identification

The scheme to estimate the unknown parameters of the control plant is as follows:

$$\theta(k) = \theta(k-1) + \left[F_p(k) - \varphi(k)^T\theta(k-1)\right], \tag{14}$$

$$K(k) = \frac{P(k-1)\varphi(k)}{\lambda+\varphi(k)^T P(k-1)\varphi(k)} \quad , \tag{15}$$

$$P(k) = \frac{P(k-1)}{\lambda}\left[I - K(k)\varphi(k)^T\right] . \tag{16}$$

The regressor vector consists of:

$$\varphi(k-1) = \begin{bmatrix} -F_p(k-1) \\ -F_p(k-2) \\ (x,y)_c(k-1) \\ (x,y)_c(k-2) \end{bmatrix} \quad . \tag{17}$$

It is important to consider, that a certain deadtime of the system shifts the inputs of the system. For the recursive algorithm, initial guesses for the parameter vector θ ($\theta(0) = [0.1 \quad 0.1 \quad 10 \quad 10]$) and the squared covariance matrix P ($P(0) = 10^5 I$) have to be placed. The forgetting factor λ is chosen to $\lambda = 0.95$. In order to provide robust estimation, the covariance matrix is reset every 500 steps. Because abrupt changes of the estimator heavily affect the controllers' output, two algorithms are run parallel. Alternate integration in the control loop ensures that the estimator being reset more recently, does not provide the data for the calculation of the manipulated variable (Fig. 5). Therewith, the risk of an unstable estimator due to non-sufficient changes of the regressor vector is avoided.

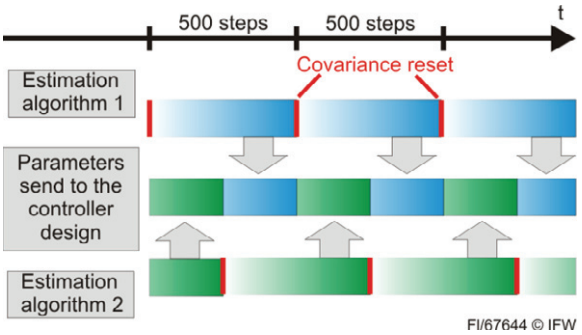

Fig, 5: Alternating covariance reset of two estimators

5. **Experimental Results**

Even though the adaptive control algorithm is capable of restricting a variety of forces acting on the cutter (e.g. feed force, feed normal force, peak force), the conducted experiment is limited to control the moving mean forces per spindle revolution.

$$F_{mean/rev} = \sqrt{F_{f,mean/rev}{}^2 + F_{fn,mean/rev}{}^2} \qquad (18)$$

This leads to spindle speed dependent plant dynamics, which are accounted by the parameter estimation.

The successful implementation of the force control loop on the basis of the magnetic guide is shown by means of a flank milling process of a step-profiled aluminum workpiece (Fig. 6). In this case, the mean force can be effectively varied by repositioning of the Z-slide in Y-direction. For safety reasons the movement within the air gap is limited to 200 µm. Every 200 µsec a new position command for the magnetic guide is sent to its control which is also running at 5 kHz. The controllers' transfer function is specified by $\omega_n = 40\,rad/s$ and $\xi = 0.95$.

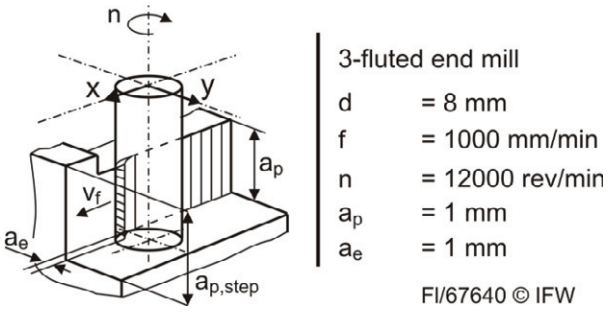

Fig 6: Test part geometry and milling parameters

Results are presented in Figure 7. Actual process force F_a- collected with a dynamometer (Kistler 9257B) - does match with the commanded force ($F_{commanded}$ = 10.5 N). The actual position of the Z-slide within the air gap of the active guide is obtained from the measurement of the displacement sensors at each electromagnet and their conversion into generalized coordinates. There is a constant change of position to maintain the desired force level. It can be identified, that the step in direction of axial depth of cut of 0.1 mm results in a lower width of cut (at 84 mm). There is hardly any overshoot in the force signal, which is partly due to lowpass characteristics of the mean force calculation. The forces of an uncontrolled milling process differ significantly from the commanded force level. Reason for changing process forces, in spite of constant cutting conditions before and after the step, may be referred to the test set-up.

In Figure 8, a process with a step change in direction of depth of cut of 0.5 mm is displayed. All other parameters, except the reference force ($F_{commanded}$ = 15.5 N), are kept constant.

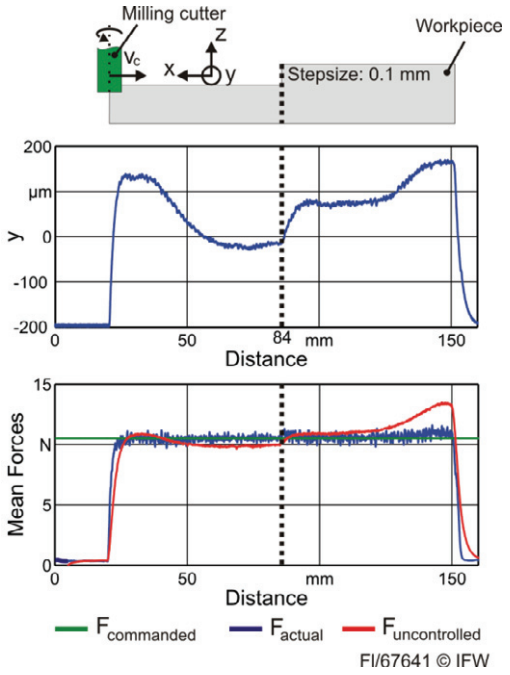

Fig. 7: Milling test of the adaptive control algorithm with a step change of 0.1 mm in the workpiece geometry

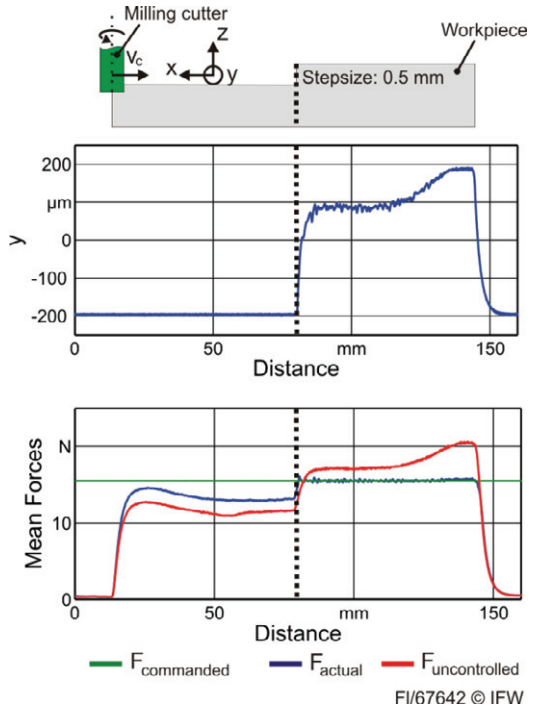

Fig. 8: Milling test of the adaptive control algorithm with a step change of 0.5 mm in the workpiece geometry

It is obvious, that relocating the spindle slide by 200 µm exhibits relatively small changes in the cutting forces and in this case, the commanded force value cannot be reached. However, big changes in cutting forces are not mandatory since the process forces should already be well known beforehand through accurate simulations.

6. **Conclusiones**

A new process chain is proposed to machine complex parts with challenging demands on surface finish and form accuracy. To ensure highest surface quality even at unknown cutting geometries and consequently unknown cutting forces, an adaptive force control of the milling process is proposed. By means of a milling machine prototype with a contactless magnetic guided spindle, a fully independent force control loop is implemented. It is shown, how the actuator and the milling process are modeled and the adaptive control algorithm is put forward. To ensure for a stable controller and reliable estimation results, the deadtime of the system is taken into account. A first result of a flank milling process is outlined.

In order to benefit from the magnetic guides' capabilities, improvements of the adaptive control system are necessary. Non-linearities in the control structure have to be taken into account to raise accuracy and robustness of the control loop.

Acknowledgements

The authors would like to thank the German Research Foundation (DFG) for funding the associated research project SFB871 (Collaborative Research Centre 871).

References

[1] Matelotti, ME., 1941. An Analysis of the milling process, Transactions of ASME 63, pp. 677-700.
[2] Masory, 0., Koren,Y., 1980. Adaptive control system for turning, Annals of the CIRP 29 (1), pp. 281-284.
[3] Masory, 0., Koren,Y., 1981. Adaptive control with process estimation, Annals of the CIRP 30 (1), pp. 373-376.
[4] Altintas, Y., 1994. Direct Adaptive Control of End Milling Process, International Journal of Machine Tools & Manufacture 34 (4), pp. 461-472.
[5] Landers, R.G., Ulsoy, A.G., Ma, Y.H., 2004. A comparison of model-based machining force control approaches. International Journal of Machine Tools & Manufacture 44 (7-8), pp. 733-748.
[6] Zhang. J.Z., Chen, J.C., 2007. The development of an in-process surface roughness adaptive control system in end milling operations. International Journal of Advanced Manufacturing Technology 31 (9-10), pp. 877-887.
[7] Denkena, B., Neuber, C.-C., Kallage, F., 2006. Machine tool with a non-contacting adaptronic slide, Adaptronic Congress, Göttingen.
[8] Denkena, B., Neuber, C.-C., Kallage, F., 2006. Adaptive Positionierung von Werkzeugmaschinenachsen mit kontaktlosen Antriebs- und Führungssystemen, 4. Paderborner Workshop ‚Entwurf mechatronischer Systeme'.
[9] Kallage, F., 2007. Einsatz magnetischer Aktor- und Führungseinheiten zur Erhöhung der Bahngenauigkeit von Hochgeschwindigkeitsfräsmaschinen, PhD Thesis, Leibniz Universität Hannover.
[10] Altintas, Y., 2000. Manufacturing Automation, Cambridge University Press.
[11] Astrom, J.K., Wittenmark, B., 1984. Computer Controlled System, Prentice Hall.